Eksploatacja i Niezawodnosc – Maintenance and Reliability
Volume 23 (2021), Issue 2
journal homepage: http://www.ein.org.pl

Article citation info:
Krešák J, Peterka P, Ambriško L, Mantič M. Friction lining coefficient of the drive friction pulley. Eksploatacja i Niezawodnosc – Maintenance and Reliability 2021; 23 (2): 338–345, http://doi.org/10.17531/ein.2021.2.13.

Friction lining coefficient of the drive friction pulley

Indexed by:
Web of Science Group

Jozef Krešák[a], Pavel Peterka[a], Ľubomír Ambriško[a], Martin Mantič[b]

[a] Faculty of Mining, Ecology, Process Control and Geotechnology, Technical University of Kosice, Park Komenskeho 14, 042 00 Kosice, Slovak Republic
[b] Faculty of Mechanical Engineering, Technical University of Košice, Letná 9, 042 00 Košice, Slovak Republic

Highlights

- The compare tests of the friction linings of mining hoisting system.
- The friction coefficient stability tests of the friction linings.
- The friction coefficient dependences on the weather conditions were analysed.
- Hardness was chosen as a representative property of the tested friction lining.

Abstract

Mine hoisting KOEPPE system or friction hoist winch work with traction pulley, the pulley rim grooves are lined. Lining has to provide a higher friction coefficient between the rope and the traction pulley. The constructors of mine hoisting machines require from the manufacturers a guaranteed appropriate and stabile value of a friction coefficient at different pressures between a rope and a friction lining under different external conditions (drought, moisture, icing, etc.). The paper presents processed measurements performed on the six samples of the friction lining (G1-G6) made of rubber and the sample of the standard used friction lining (K25). The samples (G1-G6) differ in the chemical composition of the rubber. Due to the confidentiality of the material composition of the friction linings the hardness of the lining material as a discriminator was chosen. The measured values of the friction coefficient of the rubber friction lining samples were compared with the values of the friction coefficient of the friction lining (K25) usually mounted on friction lining pulley.

Keywords

hoisting rope, friction pulley, friction lining, sliding friction coefficient.

1. Introduction

A mine hoisting system connects underground excavating areas with surface technologies; it transports extracted material, mine workers, machinery and equipment for exploitation. The main working element of mine hoisting machines is a steel wire rope, which can be wound on a drum or it can passed through a friction traction pulley. During any operation a drum hoisting system wind up one end of a hoist rope on the drum and a transport container via a cage suspension gear is gripped at the other end of the hoist rope. The rope is usually wound on the drum in one layer, but in the case of deep shafts the rope can be wound on the drum in two layers. The drum mining machines are double-acting, then the drum is divided and two hoist ropes are wound on it in two layers - upper and lower. The second frequently used type of a mine hoisting equipment is a machine with a friction pulley. These machines work with a rope passing through a friction pulley KOEPPE system or friction hoist winch, where the transport vessel travels between two horizons [5, 7]. Mańka et al. specified work of mining shaft hoist, depending on the drive type: in drum drives (rope is working in the underlap or overlap arrangement) or in drives with the frictional contact (KOEPPE system) [18]. Shirong investigated the friction coefficients between the steel wire rope and Polyvinylchloride (PVC) lining [20] and the hoisting friction conditions in a mine. The measurement shown: the friction coefficient decreases with increasing velocity or pressure and distribution of friction coefficients have a log-normal distribution [20]. Chang et al. studied wear and friction characteristics of the steel wire rope and the evolution of the tribological parameters at different friction stages [6]. Guo et al. based that force direction is deflected radially to the right. Force can be distributed into normal and friction force [11]. Ma and Lubrecht studied the local contact pressure between friction lining and steel wire rope. They developed first a 2-dimensional multigrid code based on the geometry of steel wire rope [17]. Guo et al. investigated connection between friction transmission and longitudinal rope dynamics [12]. Zhang observed when steel wire rope is working around nylon pulleys; the bending fatigue life of steel wire ropes is twice longer than that of ropes working around steel pulleys [25]. In this article we describe and compare the linings of pulleys made of rubber and plastic. Standardized method [21] described in woks [1, 10] were used in the lining hardness tests. The utilization of the new lining material and development of the new lining construction lead to optimal repair maintenance [14], higher operation reliability and long life operation of the lining [15]. Material used for manufacturing of the friction lining requires high wear resistance [8] and on the other hand high friction coefficient on the contact with steel ropes. Rubber and plastic materials used for the manufacturing of the friction linings bring specific material properties [2] proper for specific operation condition of the mining hoisting system and especially for

E-mail addresses: J. Krešák - jozef.kresak@tuke.sk, P. Peterka - pavel.peterka@tuke.sk, L. Ambriško - lubomir.ambrisko@tuke.sk, M. Mantič - martin.mantic@tuke.sk

the friction lining pulley. The most important property of the friction lining is the stability of the friction coefficient under different weather conditions and the pressure between the rope and the groove of the pulley. Reliability and safety operation of the mining hoisting system depends on the optimization of above mentioned material properties and good friction properties of the chosen material [16].

2. Theory and calculation

The transmission of force from the drive friction traction pulley to the hoist rope is performed by means of friction between the rope and the groove of the rope pulley.

The drive wheel groove is often lined with a material having a higher coefficient of friction than steel. This material called lining is inserted into the rim of the drive pulley (Fig. 1). The magnitudes of tensile forces and a circumferential force on a friction disc or a drum are described by the Euler's equation.

When F + dF > F (Fig. 1b) than the resultant horizontal force dF_H is generated and if the rope is not to slide on the pulley than this force must be in equilibrium with the friction force dT, i.e. $dF_H = dT = dN.f$. Under such a condition the circumferential driving force is transmitted from the pulley to the rope without slippage according to the principle of belt friction. The force equilibrium in the horizontal direction of the x-axis is applied due to the distribution of forces in a rectangular coordinate system:

$$dF_H = (F + dF).\cos\frac{d\alpha}{2} - F.\cos\frac{d\alpha}{2}, \tag{1}$$

after the adjustment:

$$dF_H = F.\cos\frac{d\alpha}{2} + dF.\cos\frac{d\alpha}{2} - F.\cos\frac{d\alpha}{2}. \tag{2}$$

It is possible to consider: $\cos\frac{d\alpha}{2} \approx 1$ for a differentially small angle then:

$$dF_H = dF \tag{3}$$

The force equilibrium in the vertical direction of the y-axis (Fig. 1b) is given by the equality:

$$dN = (F + dF).\sin\frac{d\alpha}{2} + F.\sin\frac{d\alpha}{2}, \tag{4}$$

after adjustment:

$$dN = F.\sin\frac{d\alpha}{2} + dF.\sin\frac{d\alpha}{2} + F.\sin\frac{d\alpha}{2} \tag{5}$$

Concerning the differentially small angle it can be speculated that:

$$\sin\frac{d\alpha}{2} \approx \frac{d\alpha}{2}, \text{ and } \quad dF.\sin\frac{d\alpha}{2} = 0 \quad \text{then:}$$

$$dN = 2.F.\frac{d\alpha}{2} = F.d\alpha\ . \tag{6}$$

Considering that: $dF_H = dT$ and $dT = dN\ .\ f$; with both $dF_H = dF$ and $dN = F.\ d\alpha$, than after the substitution:

$$dF = f.F.d\alpha \tag{7}$$

This differential equation is solved by the separation of the variables and subsequently by their integration within the defined limits of the integration variables. To be aware of the fact that the force F increases along the pulley circumference from the smallest value F_2 to the largest value F_1, which corresponds with an increase of the wrap angle on the pulley from 0 up to the resulting angle α):

$$\int_{F_2}^{F_1}\frac{dF}{F} = \int_0^{\alpha} f.d\alpha\ , \tag{8}$$

then:

$$\ln\frac{F_1}{F_2} = f.\alpha\ , \tag{9}$$

and after delogarithmization a well-known Euler`s correlation arised (10):

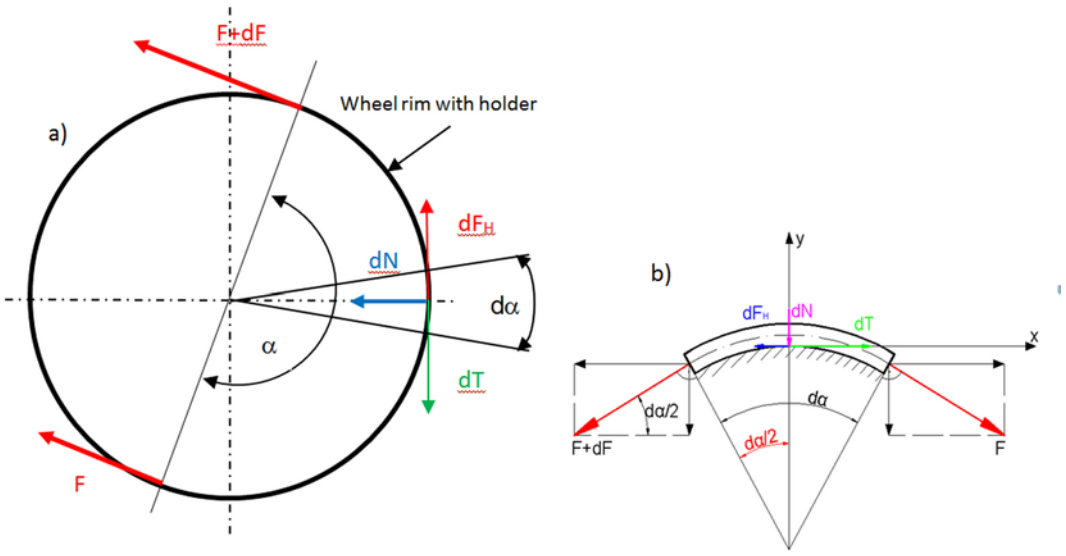

Fig. 1. Schematic force diagrams on the friction pulley a) schematic diagram of friction power transmission between friction lining and rope b) schematic diagram of friction power transmission between friction lining and rope on the elementary segment of the friction pulley

$$\frac{F_1}{F_2} = e^{f.\alpha} \tag{10}$$

During the actual hoisting the rope does not reach the state of gross slip (11):

$$F_1 = F_2.e^{f.\alpha} \tag{11}$$

where: F1 - tensile force in the digressional rope branch [N],
F2 - tensile force in the back-word running rope branch [N],
α - wrapping angle [rad],
f - friction coefficient [-].

3. Material and methods

3.1. Methodology for testing the coefficient of friction

According to the equation (11) there must be no slippage between the rope and the groove of the pulley friction lining, therefore it is necessary to know and guarantee the friction coefficient size between the rope and the friction lining. The methodology of friction force measurement is based on the principle of the equilibrium of tensile force and friction force (Fig. 1b). The tensile force (equal to the friction force) was recorded by a tensile tear tester. A measuring jig with lining samples together with a pressure force sensor was clamped in the tearing machine (Fig. 2a). According to this method the rope was inserted between two pieces of the same friction lining (Fig. 2a). The magnitude of the pressure force depends on the projection of the area of the pressed surface between the lining and the rope and on the required pressure (Fig. 2c).

The motion between the rope and the friction lining was caused by the pull of the testing machine. One of the jaws pulled the rope and the other one pulled the jig with the measured friction lining. To prevent the jig from sagging the jig arm is attached to the case by a ball joint. The case contains friction linings surrounding the rope from two sides. The rope axis passes through the imaginary axis of the jaws of the tearing machine and the box.

The force at which the motion between the rope and the friction lining took place was subtracted from the scale of the tearing machine. The starting force was considered to be the value valid for the coefficient of friction at rest (static coefficient of friction) and the force when moving was valid for the coefficient of friction in motion (dynamic coefficient of friction).

The test was performed on the non-lubricated rope and on the lubricated rope. The lubrication of the rope was performed in accordance with the Standard DIN 21258, i.e. the lubricant was applied to the rope and allowed to act at 20 °C for 16 hours. The test procedure was identical for both ropes. Due to the presence of water in mining environment the friction force between the lubricated rope and the friction lining groove was measured, while water was added to the contact area.

In the frame of the experiments the measurements were performed in order to determine the friction coefficient value for individual mixtures of the material used for the friction lining production. The friction lining samples used for the tests consisted of six types of rubber compounds (Fig. 3) and the K25 lining originally mounted on the traction pulley.

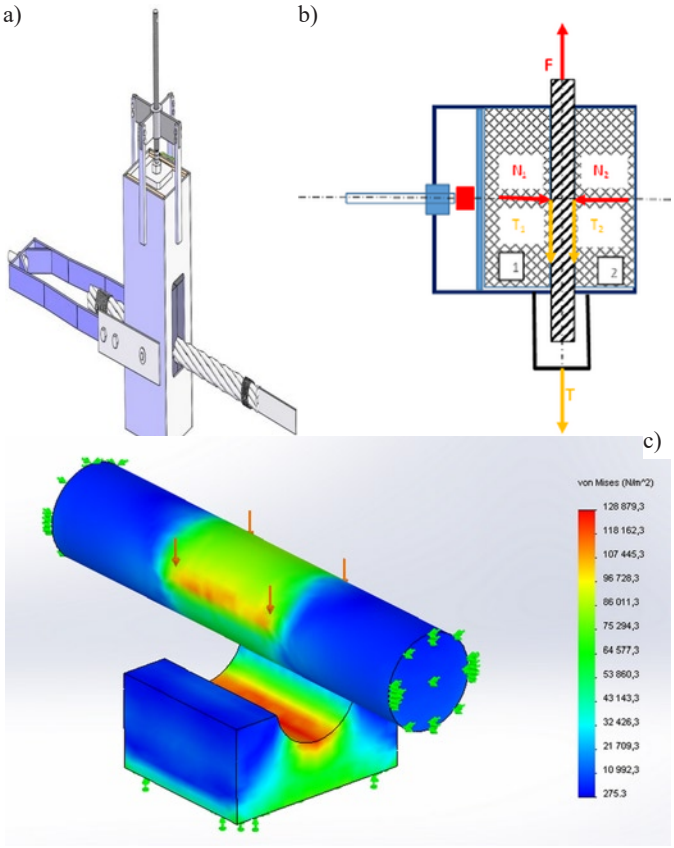

Fig. 2. The friction coefficient measurements, a) the measuring jig schema, b) the measuring jig schema with determination of N and T forces (right). c) the tension simulation model - friction lining and non-lubricated rope

The measurements were performed under the following conditions:
- friction lining and non-lubricated rope,
- friction lining and lubricated rope,
- friction lining, lubricated rope and water.

The values of the friction coefficient were measured at pressures: 1.5 MPa; 1.75 MPa; 2.0 MPa; 2.3 MPa between the rope and the friction linings.

For the calculation of the friction coefficient is valid (Fig. 2):

$$T = F \tag{13}$$

where: T – friction force [N],
F – tensile force recorded by the tear machine [N].

The equation for sliding friction is:

$$T = f.N \tag{14}$$

Fig. 3. Tested samples of the friction lining

where: N – normal force of pressure [N],
f – coefficient of sliding friction [-].

From the equilibrium of the forces according to the Fig. 2b follows:

$$T = T_1 + T_2 \tag{15}$$

where: T_1 – friction force from the lining No. 1 [N],
T_2 – friction force from the lining No. 2 [N].

If the equation (14) applies then:

$$T_1 = f.N_1 \tag{16}$$

$$T_2 = f.N_2 \tag{17}$$

where: N1 – force of the pressure on the friction lining No. 1 [N],
N2 – force of the pressure on the friction lining No. 2 [N].

The forces balance shown in the Fig. 2b:

$$N = N_1 = N_2 \tag{18}$$

After the substitution of the equations (16) and (17) in the equation (15) applies:

$$T = f.N_1 + f.N_2 \tag{19}$$

After the adjustment:

$$T = f.(N_1 + N_2) \tag{20}$$

If the equation (18) rates, then the equation (20) is:

$$T = f.(N + N) \tag{21}$$

The equation (22) for calculation of the friction coefficient is the result of the adjustment of the equation (21) and the use of the equation (13):

$$f = \frac{F}{2N} \tag{22}$$

3.2. The methodology of hardness testing

The tested rubber friction lining samples were divided following the hardness of the material. The hardness testing methodology is determined by the Standard STN EN ISO 868 and it specifies the method for determining the hardness of plastics and ebonite by indentation at which the depth of penetration of the tip is measured.

The Shore method is empirical; it is set for control purposes mostly. The hardness is inversely proportional to the tip intrusion. The tip intrusion depends on the modulus of elasticity and the visco - elastic properties of the tested material. The tip (made of hardened steel rod) has the shape of a beveled cone with an apex angle of 35° ± 0.25°, Ø 0.79 ± 0.03 mm [20].

The samples hardness was measured on five different places: the distance (Fig.4a) from the sample's edge min. 9 mm, the distance between punctures min. 6 mm (Fig. 4b) [1, 9].

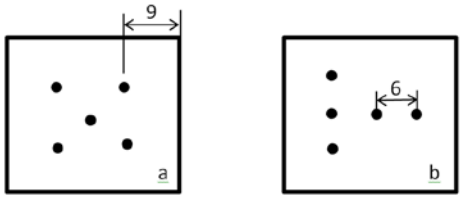

Fig. 4. Minimum distances in millimeters for the placemen of the punctures [1] A) distance of the punctures from the edge of the sample, B) distance between the punctures

4. Results

4.1. Measurement of the samples hardness

Hardness was chosen as a representative material property of the tested friction lining samples. The measured results (values for 5 punctures and average values of Shore hardness of rubber samples) are shown in the Table 1.

Table 1. Measured values of the Shore hardness of rubber samples G1 - G6 and sample K25

puncture/sample	K25	G1	G2	G3	G4	G5	G6
1	87,1	96,6	91,1	90,4	83	77	89,8
2	87,7	95,1	90,6	91,1	83	76,9	91,5
3	86,7	94,6	91,6	91,4	82,1	79,9	91,7
4	87,2	95,8	90,3	91,2	85,8	79,9	90,9
5	85,8	95	90,3	87,6	86,9	78,7	92,2
average	86,9	95,4	90,8	90,3	84,2	78,5	91,2

The maximum average value of the Shore hardness A / 15: 95.4 was measured out on the sample G1; the sample G5 showed the minimum average value of A / 15: 78.5.

The IRHD hardness measurements were also performed on the samples. The course of values of the hardness shows the Table 2. Both hardness measurements issue that the sample G5 has the softest material.

Table 2. Measured the IRHD hardness values of the rubber samples

sample	K25	G1	G2	G3	G4	G5	G6
IRHD	99,1	98,3	96,2	98,4	98,3	95,1	97,3

4.2. Measurement of the friction coefficient

The Fig. 5. shows the course of the friction coefficient measurement. The measuring jig was inserted between the jaws of the shredder. The rope sample was attached to one jaw and a lined fixture was attached to the other jaw. The defined pressure between the rope and the lining was developed by the pressure screw and then the moment, when it comes to the shift between the rope and the friction lining, was monitored.

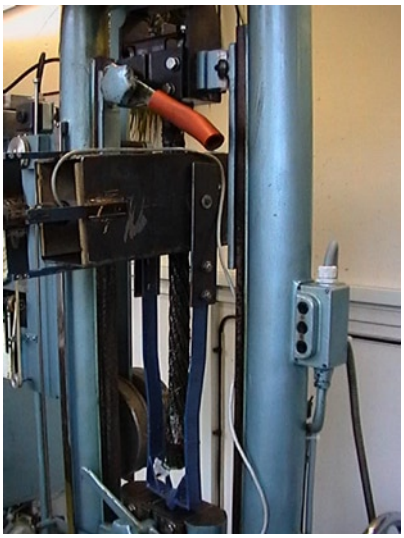

Fig. 5. The shredder and the measuring jig with the rope

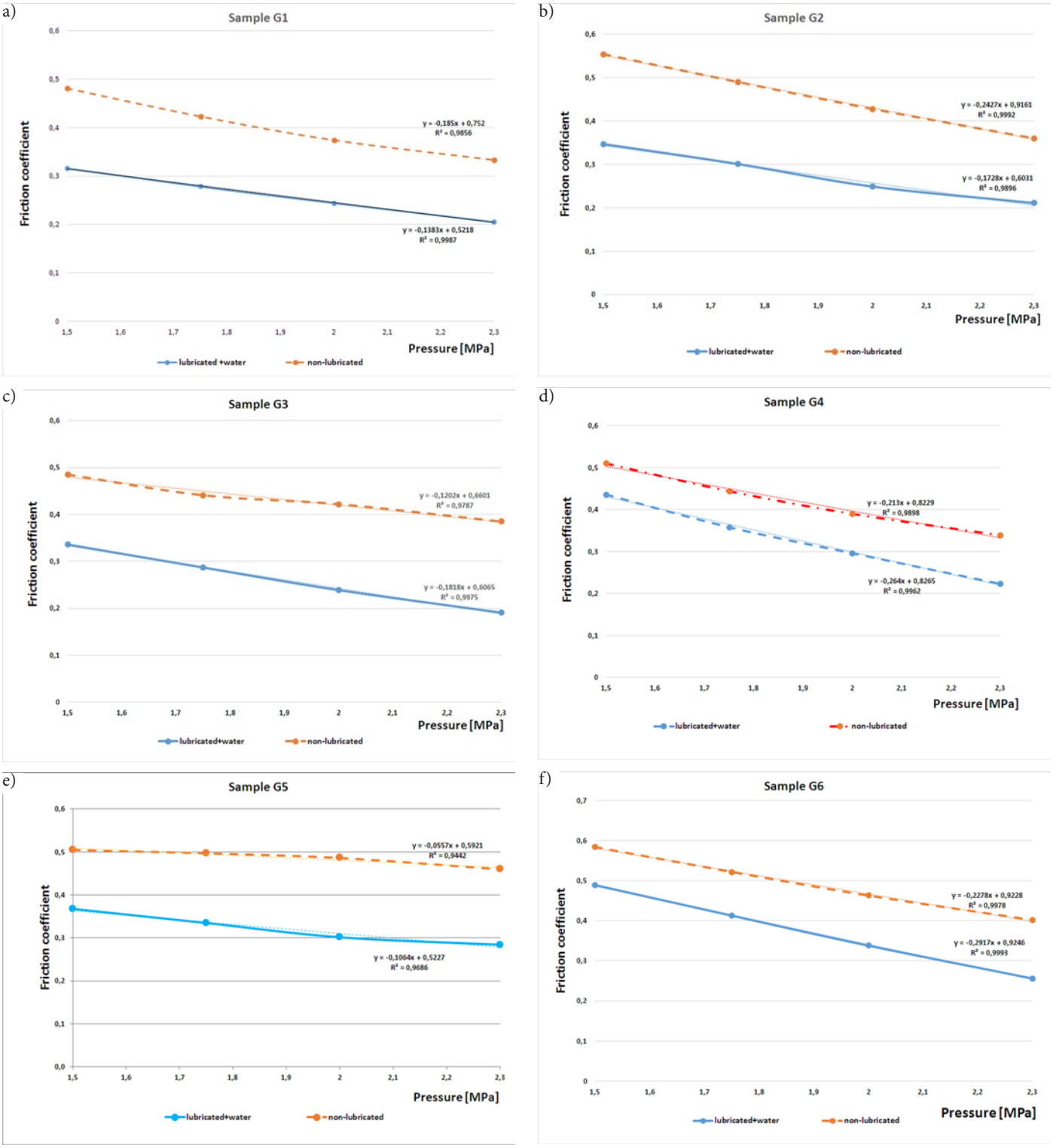

Fig. 6. The graphic dependences of the friction coefficient on the pressure magnitude between the lining and the rope; a– sample G1; b– sample G2; c– sample G3; d– sample G4; e– sample G5; f– sample G6; g– sample K25

Fig. 6. a-i show the graphical dependences and the courses of the average values magnitude of the friction coefficients (from four measurements) depending on the magnitude of the pressure exerted between the rope and the friction lining, the condition of the ropes (non-lubricated, lubricated) and the presence of water.

5. Discussion

The rate of the perpendicular and parallel acting forces on the contact between two sliding bodies is defined as a friction coefficient [4]. Blau defined six categories of the testing devices for measuring of the friction coefficient in the laboratory condition [4]. Laboratory tests used for characterisation of the friction coefficient were made by many authors. They presented results of the basic friction tests made by gravitation based devices, direct linear force measurement devices or oscillation decrement devices. The test equipment used for above mentioned measurements can be defined as a tension wrap device according [4]. The measurement jig (Fig. 2) used for determination of the friction coefficient provide laboratory tests in the conditions close to real. Creep characteristics and dynamic friction transmission between friction lining and steel wire ropes were in situ investigated by Wang et al [23]. Wang et al. focused on correlation between effective

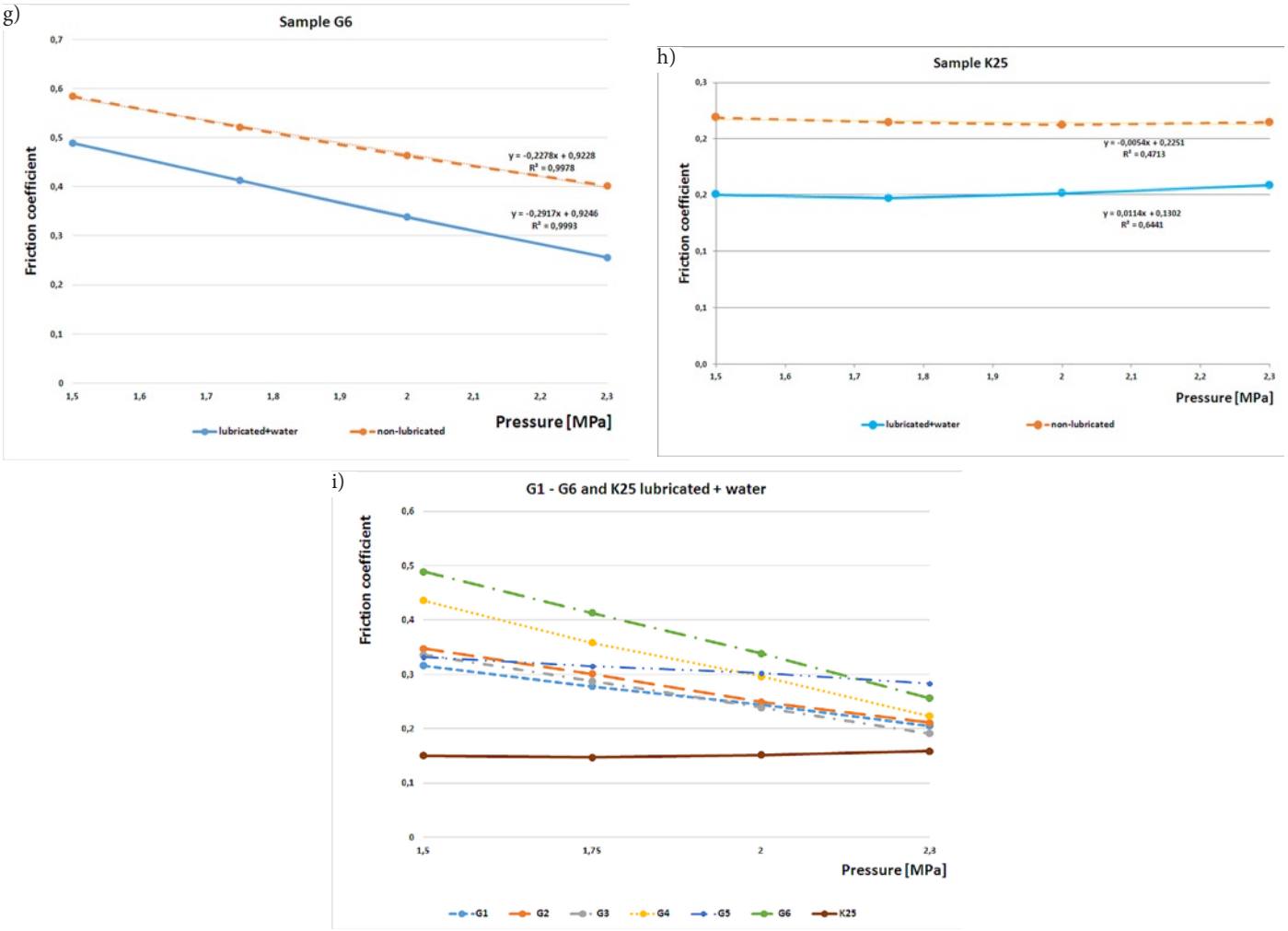

Fig. 6. [continued] g– sample K25; h – non lubricated: G1 - G6 and K 25; i– lubricated + water: G1 - G6 and K25

load, speed acceleration and deceleration to active slip angle, creep amplitude and creep velocity in process of vertical mining transport [23]. Dynamic contact characteristics between friction lining and steel wire rope were investigated by Wang et al. [22]. Wang et al. demonstrated effect of hoisting parameters on wear process of the lining and possibility of the gross slip [22]. Results presented in publications [22, 23] are focused on global effect of the hoisting process. Argatov and Chai studied effect of a variable friction coefficient on the fretting wear in conditions of gross sliding [3]. Argatov and Chai designed an asymptotic model for the progress of the contact area between the contacting surfaces [3]. The Figures 6 a-i are presented the measurements of the contact characteristics between the steel wire rope and the linings; friction coefficient of various rubber lining materials in various contact pressure is determined as well. Friction coefficients on the contact between the rubber block and smooth steel surface were investigated by Yamaguchi et al [24]. They focused on the effect of height and orientation of the rubber block on the friction coefficient [24]. Sliding friction characteristics of the water lubricated rubbers studied Ido et al. [13]. They focused on the surface topography of the rubber blocks and its effect on wet sliding friction characteristics [13]. Friction behaviour between glass plate and rubber was investigated by Nishi et al [19]. Rheological properties and effect of friction greases on friction between steel wire rope and fiction lining studied Feng at al. [9]. Feng et al. focused on the temperature and friction coefficient changes in the friction process and rheological properties of the friction-enhancing grease [9]. The results of the measurement manifest that regardless of the weather conditions (Fig. 6h and 6i) the friction lining samples made of rubber (G1-G6) have a higher friction coefficient than the sample K25. The samples comparison in terms of pressure between the rope and the friction lining indicates that the K25 friction coefficient does not change its value depending upon pressure (Fig. 6g). The course of the measured values of the friction coefficient of the friction lining K25 is much parallel to the pressure axis (Fig. 6g). The higher measured values of the friction coefficient for the friction linings G1 - G6 are evident pursuant to the comparison of all individual friction linings measurements (Fig. 6h and 6i). The significant changes in the values of the friction coefficient are visible, which in the case of friction linings G1 - G6 decreases considerably with increasing pressure (Fig. 6h, i). The decreasing course is identical with both ropes - non-lubricated and lubricated. From the samples G1 - G6 only the sample G5 has the course of the dependence of the friction coefficient on pressure similar to the sample K25, but the reached values of the friction coefficient are doubled.

The hardness values of the samples G4 and G5 are very similar to each other according to the Shore's hardness measurement method; the samples G4 and G5 are closest to the hardness value of the comparison sample K25 (Fig. 7).The sample G5 was chosen to be compared with the sample K25 due to the same trend of the course of the friction coefficient (Fig. 8, 9). Table 3 introduces directives and heading angles of the compared samples.

The trend lines overlayed by the values of the friction coefficient of the sample K25 with the non-lubricated and the lubricated rope are almost parallel to the x-axis (Fig. 8, 9). The sample made of K25 hardly changes the value of the friction coefficient depending on the value of the pressure between the friction lining and the rope. Likewise, the lines overlayed by the values of the friction coefficient of the sample G5 with the non-lubricated and the lubricated rope have the analogical course with the x-axis as well as the trend. The heading angles are

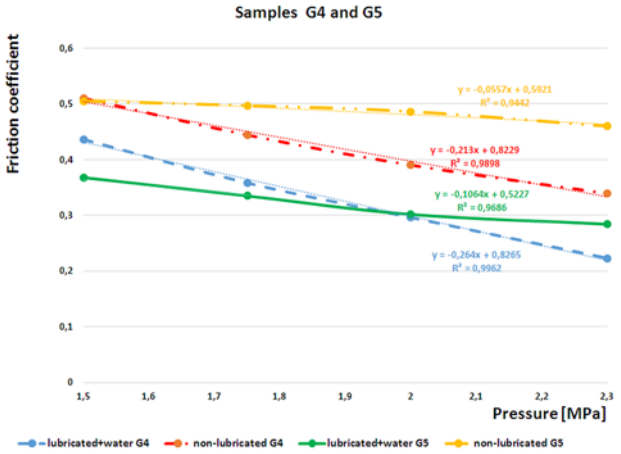

Fig. 7. Trends of the friction coefficient of the samples G4, G5 non-lubricated and lubricated + water

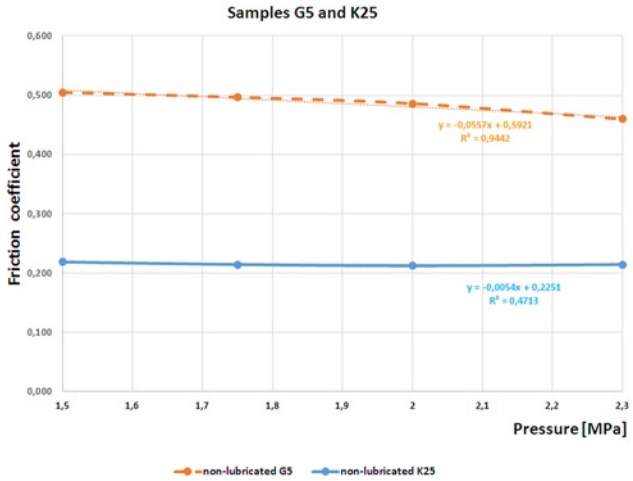

Fig. 8. Trends of the friction coefficient of the unlubricated samples G5 and K25

Table 3. Directives and heading angles α of the friction coefficient lines (Fig. 8 and 9)

Test condition	Sample K 25		Sample G5	
	Directive	Angle α	Directive	Angle α
non-lubricated rope	-0.0054	-0°18"	-0.0557	-3°11"
lubricated rope + water	0.0114	+0°39"	-0.1064	-6°4"

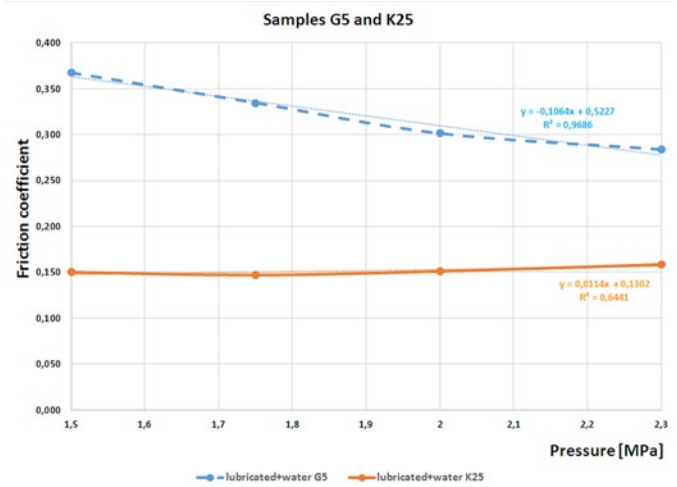

Fig. 9. Trends of the friction coefficient of the samples G5 and K25 lubricated +water

slightly larger than the angles of the sample K25, but they decrease with increasing pressure value (Fig. 8, 9).

6. Conclusion

The measured results of the friction coefficient show that all the rubber samples (G1 – G6) of the friction lining have a higher value of the friction coefficient than the friction lining K25. This applies to the entire pressure range between the rope and the friction lining, which is designated by the manufacturer of the towing equipment.

The trend of the values of the friction coefficient of the lining K25 is almost parallel to the axis of pressure (Fig. 6h and i, Fig. 8, 9). This means that the value of the friction coefficient changes very little with increasing pressure between the rope and the friction lining.

The friction lining G5 has a similar trend of the friction coefficient as the friction lining K25 (Fig. 8, 9). The rubber lining G5 shows a larger decrease of the friction coefficient value depending on the pressure than the lining K25. The values of the coefficient factor are significantly higher than the K25 has reached in the whole pressure range.

In terms of hardness the sample G4 is the closest one to the hardness values of the lining K25. Comparing it with the sample G5 (the lowest hardness of all rubber samples) the values of the friction coefficient of the sample G4 decrease significantly faster than it is with the sample G5 (Fig. 7).

Acknowledgments

Supported by the Scientific Grant Agency (VEGA) of the Ministry of Education of the Slovak Republic and the Slovak Academy of Sciences, Grant No. VEGA 1/0075/20.

References

1. Ambriško Ľ. Determination of the abrasion resistance and the hardness of rubber covering layers. International Multidisciplinary Scientific GeoConference Surveying, Geology and Mining, Ecology and Management, SGEM conference proceedings, Bulgaria 2018; 18 (1.3): 255-262, https://doi.org/10.5593/sgem2018/1.3/S03.033
2. Andrejiova M, Grincova A, Marasova D. Analysis of tensile properties of worn fabric conveyor belts with renovated cover and with the different carcass type. Eksploatacja i Niezawodnosc - Maintenance and Reliability 2020; 22 (3): 472-481, https://doi.org/10.17531/ein.2020.3.10.
3. Argatov I I, Young S. Chai Y S. Fretting wear with variable coefficient of friction in gross sliding conditions. Tribology International 2021; 153: 106555, https://doi.org/10.1016/j.triboint.2020.106555.
4. Blau P J. The significance and use of the friction coefficient. Tribology International 2001; 34: 585-591, https://doi.org/10.1016/S0301-679X(01)00050-0.
5. Chang X, Peng Y, Zhu Z, Gong X. Breaking failure analysis and finite element simulation of wear-out winding hoist wire rope. Engineering Failure Analysis 2018; 95: 1-17, https://doi.org/10.1016/j.engfailanal.2018.08.027.
6. Chang X D, Peng Y X, Zhu Z C, Zou S Y, Gong X S, Xu C M. Evolution Properties of Tribological Parameters for Steel Wire Rope under Sliding Contact Conditions. Metals (Basel) 2018; 8 (10): 743, https://doi.org/10.3390/met8100743.

7. Čereška A, Zavadskas E K, Bucinskas V, Podvezko V, Sutinys E. Analysis of Steel Wire Rope Diagnostic Data Applying Multi-Criteria Methods. Applied Sciences 2018; 8 (2): 260, https://doi.org/10.3390/app8020260.
8. Dzierwa A, Gałda L, Tupaj M, Dudek K. Investigation of wear resistance of selected materials after slide burnishing process. Eksploatacja i Niezawodnosc - Maintenance and Reliability 2020; 22 (3): 432-439, https://doi.org/10.17531/ein.2020.3.5.
9. Feng C, Zhang D, Grecov D, Chen K. Effect of rheological properties of friction- enhancing greases on the friction between friction lining and wire rope. Tribology International 2020; 144: 106143, https://doi.org/10.1016/j.triboint.2019.106143.
10. Grinčová A, Marasová D. Experimental research and mathematical modelling as an effective tool of assessing failure of conveyor belts. Eksploatacja i Niezawodnosc - Mainteneance and Reliability 2014; 16 (2): 229-235.
11. Guo Y, Zhang D, Yang X, Feng C, Ge S. Experimental research on effect of wire rope transverse vibration on friction transmission stability in a friction hoisting system. Tribology International 2017; 115: 233-245, https://doi.org/10.1016/j.triboint.2017.05.033.
12. Guo Y, Zhang D, Chen K, Feng C, Ge S. Longitudinal dynamic characteristics of steel wire rope in a friction hoisting system and its coupling effect with friction transmission. Tribology International 2017; 119: 731-743, https://doi.org/10.1016/j.triboint.2017.12.014.
13. Ido T, Yamaguchi T, Shibata K, Matsuki K, Yumii K, Hokkirigawa K. Sliding friction characteristics of styrene butadiene rubbers with varied surface roughness under water lubrication. Tribology International 2019; 133: 230-235, https://doi.org/10.1016/j.triboint.2019.01.015.
14. Knopik L, Migawa K. Semi-Markov system model for minimal repair maintenance. Eksploatacja i Niezawodnosc - Maintenance and Reliability 2019; 21 (2): 256-260, https://doi.org/10.17531/ein.2019.2.9.
15. Kosobudzki M, Stańco M. Problems in assessing the durability of a selected vehicle component based on the accelerated proving ground test. Eksploatacja i Niezawodnosc - Maintenance and Reliability 2019; 21 (4): 592-598, https://doi.org/10.17531/ein.2019.4.8.
16. Li Y H, Liang X J, Dong S H. Reliability optimization design method based on multi-level surrogate model. Eksploatacja i Niezawodnosc - Maintenance and Reliability 2020; 22 (4): 638-650, https://doi.org/10.17531/ein.2020.4.7.
17. Ma W, Lubrecht A A. Detailed contact pressure between wire rope and friction lining. Tribology International 2016; 109: 238-245, https://doi.org/10.1016/j.triboint.2016.12.051.
18. Mańka E, Słomion M, Matuszewski M. Constructional Features of Ropes in Functional Units of Mining Shaft Hoist. Acta Mechanica et Automatica 2018; 12 (1): 66-71, https://doi.org/10.2478/ama-2018-0011.
19. Nishi T, Takeshi Yamaguchi T, Shibata K, Hokkirigawa K. Influence of unforced dewetting and enforced wetting on real contact formation and friction behavior between rubber hemisphere and glass plate during contacting and sliding processes. Tribology International 2020; 141: 105921, https://doi.org/10.1016/j.triboint.2019.105921.
20. Shirong G. The friction coefficients between the steel rope and polymer lining in frictional hoisting. Wear 1992; 152 (1): 21-29, https://doi.org/10.1016/0043-1648(92)90201-I.
21. STN EN ISO 868: 2003, Plastics and ebonite. Determination of indentation hardness by means of a durometer (Shore hardness).
22. Wang D, Li X, Wang X, Shi G, Mao X, Wang D. Effects of hoisting parameters on dynamic contact characteristics between the rope and friction lining in a deep coal mine. Tribology International 2016; 96: 31-34, https://doi.org/10.1016/j.triboint.2015.12.019.
23. Wang D, Zhang D, Mao X, Peng Y, Ge S. Dynamic friction transmission amd creep characteristics between hoisting rope and friction lining. Engineering Failure analysis 2015; 57: 499-510, https://doi.org/10.1016/j.engfailanal.2016.03.006.
24. Yamaguchi T, Katsurashima Y, Hokkirigawa K. Effect of rubber block height and orientation on the coefficients of friction against smooth steel surface lubricated with glycerol solution. Tribology International 2017; 110: 96-102, https://doi.org/10.1016/j.triboint.2017.02.015.
25. Zhang D, Chen K, Jia X, Wang D, Wang S, Luo Y, Ge Y. Bending fatigue behaviour of bearing ropes working around pulleys of different materials. Engineering Failure Analysis 2013; 33: 37-47, https://doi.org/10.1016/j.engfailanal.2013.04.018.